

Magnetic Force Investigation of High- T_c Superconducting Bulk over Permanent Magnet Railway under Different Lateral Offsets with Experimental Methods

Yiyun Lu^{1*}, Daqing He¹, Minxian Liu²

¹Luoyang Institute of Science and Technology, Luoyang, China

²School of Computer Science and Technology, Southwest University of Science and Technology, Mianyang, China

Email: *luyiyun6666@vip.sohu.com, liukey_sjtu@263.net

Received March 26, 2013; revised April 28, 2013; accepted May 23, 2013

Copyright © 2013 Yiyun Lu *et al.* This is an open access article distributed under the Creative Commons Attribution License, which permits unrestricted use, distribution, and reproduction in any medium, provided the original work is properly cited.

ABSTRACT

The magnetic levitation transportation system is one of the potential applications of high- T_c superconducting (HTS) maglev system. The prototype HTS magnetic levitation system is composed of one HTS bulk and a permanent magnet railway (PMR). The maglev transportation system performance is influenced by the maximum levitation force, the maximum guidance force and the maximum of external applied magnetic flux density. The applied magnetic field distribution also needs to be considered carefully. In the paper, the magnetic levitation force of cylindrical HTS bulk over PMR is experimentally studied. During the experiment, symmetrical PMR and Halbach PMR are used separately. The levitation force-gap loops of different lateral offset of the HTS bulk above PMRs are obtained experimentally. The results show that the HTS bulk levitation performance is tightly relative to the external applied magnetic field distribution. The maximum magnetic levitation forces of HTS bulk above symmetrical PMR decrease linearly with the lateral offset increasing. When the lateral offset changes from 0 mm to 25 mm, the maximum magnetic levitation forces of HTS bulk above Halbach PMR increase with the lateral offset increasing. When the lateral offset exceeds the center of the Halbach PMR by 25 mm, the maximum force decreases rapidly with the increase of the lateral offset of the bulk sample.

Keywords: Bulk; HTS; Permanent Magnetic Railway; Lateral Offset

1. Introduction

The high- T_c superconducting (HTS) bulk can stably levitate above permanent magnet (PM) without any complex controlling system. Based on the inherent stability characteristics, HTS bulk has more potential applications in many fields, especially in HTS maglev vehicle [1-4]. Recently years the new superconductor's theory and materials technology development (such as Fe-based superconductor) may enhance the HTS potential for various engineering applications [5]. A most popular application of HTS bulk is magnetic levitation transportation system. The magnetic levitation force is one important factor for the HTS maglev vehicle optimization design. The prototype HTS magnetic levitation transportation system is composed of HTS bulk and permanent magnetic railway (PMR). Many researching works have been done to investigate the performance of the magnetic levitation force of HTS bulk over PMR. Deng studied the cost per-

formance of YBCO bulks over two types of PMR by magnetic levitation force [6]. Dr. Zhang has researched magnetic levitation force relaxation characteristics of YBCO bulk over PM under different temperatures [7]. Liu has researched magnetic levitation force decay characteristics of YBCO bulk over PMR while the bulk is applied with external AC magnetic fields [8]. Lu experimentally measured magnetic levitation force stiffness of YBCO bulk arrays over two types PMR and researched the magnetic levitation performance of YBCO bulk over PMR using a 3D-modeling method [9,10].

During the HTS bulk maglev system optimization design, many researchers focus on the maximum magnetic levitation force of HTS bulk. As we all know, the levitation performance of HTS bulk over PMR is tightly related to its critical current density, flux pinning ability and the maximum value of applied magnet fields induced by the PMR. Many practice prototype maglev test vehicles involve HTS bulk arrays and PMR. How to arrange HTS bulk arrays above PMR and magnetic field distribu-

*Corresponding author.

tion induced by the PMR also needs to be carefully considered. For cylindrical HTS bulk arrays, two kinds of arrangement are often be used, as **Figures 1(a)** and **(b)** show. The first man-loading HTS magnetic levitation test vehicle used on-boarding 48 low temperature vessels. Each contains one YBCO bulk array of **Figure 1(b)** for magnetic forces supply [11]. Seldom report has been seen in the use of HTS bulk arrays of **Figure 1(c)**.

In the paper, the influence of applied magnetic field distribution on magnetic levitation force of YBCO bulk is studied experimentally. The experiment is carried out by the method that the magnetic levitation force-gap curves of YBCO bulk with different lateral offsets over PMR are measured. One cylindrical YBCO bulk of 30 mm in diameter and 15 mm in thickness is used. During the experiment, symmetrical PMR and Halbach PMR are used separately. The lateral offset of the YBCO bulk over PMR increases from 0 mm to 30 mm by the step size of 5 mm. The experimental results show that the maximum magnetic levitation forces of the YBCO bulk which corresponding to different lateral offsets are tightly related to the applied magnetic field distribution. For the symmetrical PMR, the maximum levitation force of the YBCO bulk decreases linearly with the lateral offset increasing. For the Halbach PMR, when the lateral offset changes from 0 mm to 25 mm, the maximum levitation force of the YBCO bulk increases with the lateral offset increasing. When the lateral offset exceeds the center of the Halbach by 25 mm, the maximum levitation force decreases rapidly with the increase of the lateral offset of the YBCO bulk.

2. Experimental Procedure

As **Figure 2** shows, one YBCO bulk is fixed at the bottom of the LN₂ Dewar vessel which is above the PMR with c-axis oriented perpendicular to the surface of the PMR. The YBCO bulk is 30 mm in diameter and 15 mm in thickness. The LN₂ cryogenics vessel is located below a rigidity epoxy plate with two levitation force sensors.

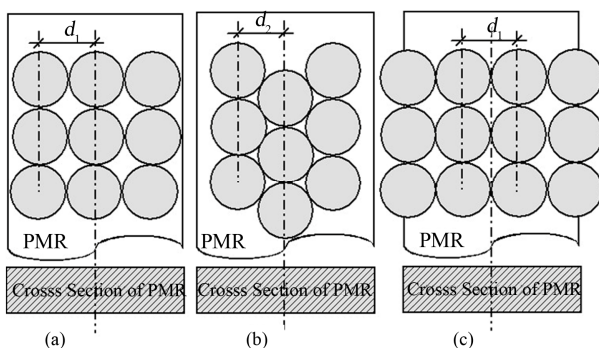


Figure 1. Schematic diagram of three kinds of HTS bulk arrays over PMR. (a) HTS bulk matrix-T₁ array; (b) HTS bulk stagger array; (c) HTS bulk matrix-T₂ array.

The PMR top surface center is taken as the origin of rectangular coordinates. The cryogenics vessel can be moved freely in the vertical direction by one z-axis servomotor. During the experiment, the PMR is located at the x-y platform which connects with two servomotors controlled by computer. The PMR could move along x-axis and y-axis separately by those two servomotors. As **Figure 2** (5) shows, the levitation force acting on the YBCO bulk is transferred to the LN₂ vessel and then transferred to two levitation force sensors.

During the experiment, two types of PMR are used separately. One is symmetrical PMR, the other is Halbach PMR. **Figure 3** shows the structure of the two types PMR and its magnetic field distribution. The symmetrical PMR is composed of two NdFeB PMs and one pure iron. The center pure iron is used for concentrating the magnetic flux. The cross section of the symmetrical PMR is 90 mm in width and 40 mm in height. The Halbach PMR is composed of five NdFeB PMs. Different with symmetrical PMR, Halbach PMR uses PM for concentrating the magnetic flux. The cross section of the Halbach PMR is 80 mm in width and 20 mm in height.

In the experiments, the magnetic levitation force-gap loops of the YBCO bulk are successfully measured. **Figure 4** shows the schematic diagram of the measuring progress. During the experiments the bulk sample is cooled in zero-field cooling case at the position A above the PMR where the external magnetic flux density is about zero. The magnetic levitation force-gap loops are measured with different lateral offset. For each loop measuring, firstly, the PMR is moved in the horizon plane along x-axis to a special lateral offset by the x-axis

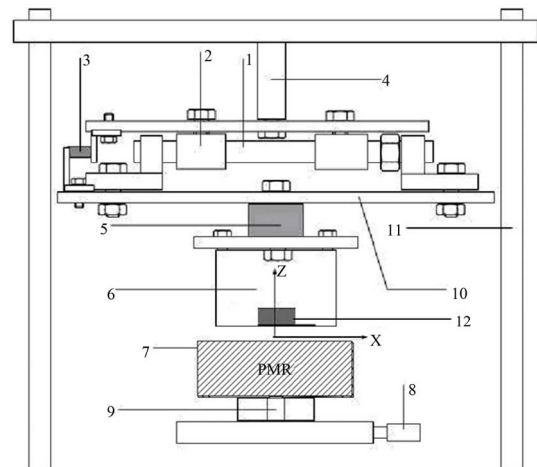


Figure 2. Sketch of the apparatus measuring the magnetic forces of the YBCO bulk. (1) Two parallel guiding slide-rods; (2) guiding slide bushing; (3) guidance force sensor; (4) z-axis servo-motor; (5) two levitation force sensors; (6) LN₂ vessel; (7) PMR; (8) x-axis servo-motor; (9) y-axis servo-motor; (10) epoxy plate; (11) support frame; (12) single YBCO bulk.

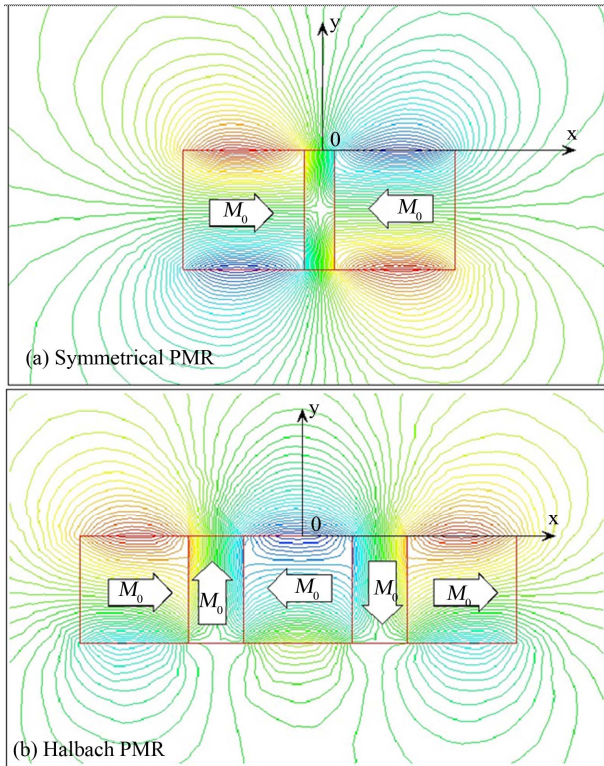


Figure 3. The magnetic field distribution of the PMRs. (a) Symmetrical PMR; (b) Halbach PMR.

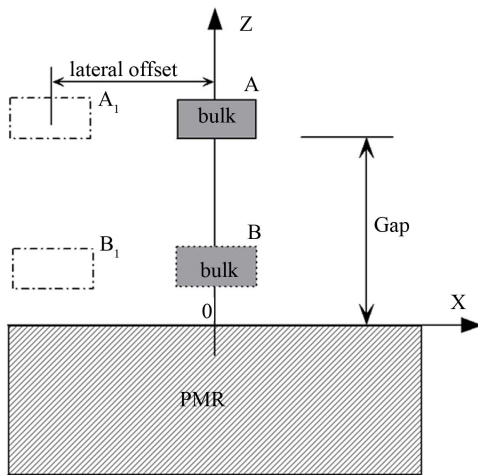


Figure 4. Sketch of the YBCO bulk magnetic force-gap loops measurement with special lateral offset.

servo-motor (see Figure 2); after the YBCO bulk transits to the superconducting state, the bulk sample is vertically brought down from position A₁ to position B₁ with the specific lateral offset above the PMR (see Figure 4). The moving velocity of the YBCO bulk is equal to 1 mm/s. After the bulk sample arrives at position B₁, it is brought away back to position A with the same velocity. During the experimental progress, the lateral offset changes from 0 mm to 30 mm with the step size equal to

5 mm. Each lateral offset step corresponds to one magnetic levitation force-gap loop.

3. Experimental Results and Discussion

Figure 5 shows the levitation force-gap loops of the YBCO bulk in the zero-field cooling case above the symmetrical PMR with different lateral offset.

From the results, we can see that all the levitation force-gap loops exhibit some hysteresis. This can be explained by the characteristics of HTS magnetic hysteretic effects. When the bulk sample is moved gradually to the top of the PMR, the applied magnetic flux density also increased gradually. The magnetic flux began penetrate into the sample body from surface. The trapped flux was pinned in the bulk interior. As the result, the YBCO bulk was magnetized. When the YBCO bulk arrived at the lowest position B and began move back to the initial position A, the applied magnetic flux density began decrease, the inverse screen currents was induced. As a result, some trapped magnetic flux began escape from it's pinning center. Macroscopically, the trapped magnetic flux density decreased and shows some hysteretic effects of the levitation force curve.

Figure 5 also shows that with the decrease of the gap, the difference of levitation forces which corresponding to different lateral offset of the YBCO bulk becomes larger. Furthermore, for the same gap, the levitation forces decreases with the increase of lateral offset of the bulk sample. From Figure 5, we can see that all the levitation force-gap loops is above zero. When YBCO bulk transits to superconducting state and begin to move vertically down to the PMR, the magnetic flux then begins to penetrate into the body of the YBCO bulk. With the bulk sample getting closer to the PMR gradually, the penetrating effects become stronger and then parts of the magnetic levitation force now become negative, which

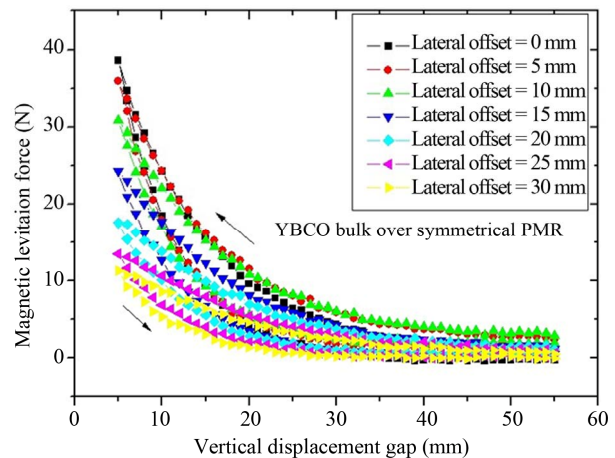


Figure 5. Magnetic levitation force-gap loops of YBCO bulk over symmetrical PMR with different lateral offset.

means pulling force. When the YBCO bulk arrives at the lowest position B and begin to move back vertically to the position A, most of the penetrating magnetic flux will be frozen into the superconducting body because of flux pinning effects. That is one of the reasons why levitation force-gap loops exhibits some hysteresis.

Figure 6 shows the levitation force-gap loops of the YBCO bulk in zero-field cooling case above the Halbach PMR with different lateral offset. From **Figure 6** we can see that all the levitation force-gap loops exhibit some hysteresis, this is similar to the YBCO bulk over the symmetrical PMR. When the lateral offset increases from 0 mm to 25 mm gradually, the hysteresis increases either; when the lateral offset is larger than 25 mm, the hysteresis of force-gap loop decreases instead. This is different to the case of YBCO bulk over the symmetrical PMR. In order to show clearly the maximum levitation forces of the YBCO bulk above the symmetrical PMR and Halbach PMR, we draw the maximum levitation force curves which corresponding to different lateral offsets, as shown in **Figure 7**.

Figure 7 shows that the maximum levitation force of YBCO bulk decreases monotonously with the increase of lateral offset while the bulk sample above the symmetrical PMR. If the YBCO bulk is above the Halbach PMR, the maximum levitation force of the bulk sample changes non-monotonously with the increasing of lateral offset. When the lateral offset increases from 0 mm to 25 mm, the maximum levitation force increases monotonously; when the lateral offset is larger than 25 mm, the maximum levitation force decreases rapidly. This is different to the case of YBCO bulk over the symmetrical PMR.

This can be interpreted by the applied magnetic fields distribution. While the lateral offset of the bulk sample over the Halbach PMR increases, the applied magnetic flux density increases too. This is because of the structure of the Halbach PMR. **Figure 3** shows the magnetic

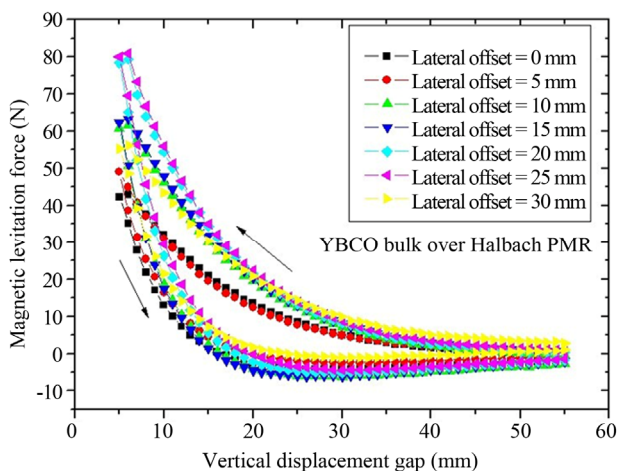


Figure 6. Magnetic levitation force-gap loops of YBCO bulk over the Halbach PMR with different lateral offset.

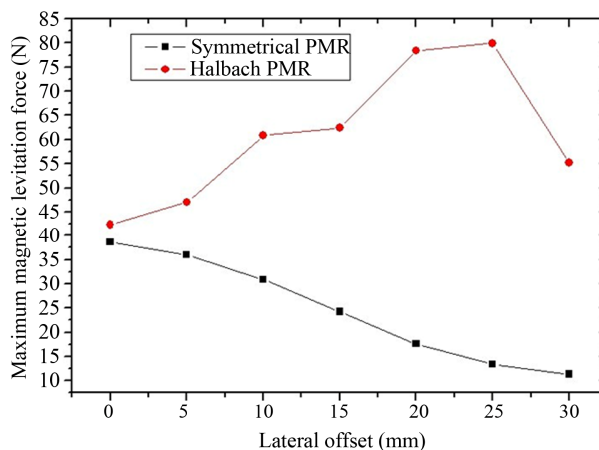


Figure 7. Maximum levitation forces of YBCO bulk above two types of PMR with different lateral offset.

fields distribution induced by the Halbach PMR. When the lateral offset is larger than 25 mm, the applied magnetic flux density began decrease and the maximum levitation force decreases. We call the Halbach PMR as double pole PMR, compare with symmetrical monopole PMR.

The experimental results also show that the magnetic levitation force characteristics of YBCO bulk above PMR are closely related to the applied magnetic field distribution induced by the PMR.

From the discussion above we can get the conclusion that, in a maglev system applied of symmetrical PMR, the bulk should be located close to the center of the PMR, which means the HTS bulk stagger array is better than the other array arrangement (see **Figure 1**). On the contrary, for the maglev system applied of Halbach PMR, the HTS bulk matrix array is better than stagger array and forth more, HTS bulk should be located close to the position of lateral offset equal to 25 mm instead of the center of the PMR.

4. Conclusions

In the paper, the levitation force-gap loops of one cylindrical shape YBCO bulk over two types of PMR with different lateral offsets are experimentally measured. The experimental results show that the maximum levitation force will decrease monotonously with the increase of lateral offset of the bulk HTS over symmetrical PMR. For Halbach PMR, there is a value of the lateral offset of the YBCO bulk, when the lateral offset increases from 0 mm to the value (in the paper, the value is about 25 mm), the maximum levitation force increases monotonously; when the lateral offset exceeds the value, the maximum levitation force begins decrease rapidly.

The levitation performance is tightly related to applied magnetic fields distribution. With certain applied magnetic fields, the arrangement of YBCO bulk arrays need consider carefully. The optimization of magnetic levita-

tion transportation system composed of HTS bulk arrays and PMR not only consider the applied magnetic field enhancement, but also the applied magnetic field distribution. For symmetrical PMR, the HTS bulk stagger array arrangement may better than others (as is showed in **Figure 1(b)**); for Halbach PMR, the HTS bulk matrix array is better than stagger array arrangement (as is showed in **Figure 1(c)**).

5. Acknowledgements

This work is supported by the Fund of National Natural Science Foundation of China (No. 11205080). All the experimental equipments are supplied by Applied Superconductivity Labs, Southwest Jiaotong University, and the authors also benefit from helpful discussions with Prof. Jiasu Wang. So, we wish to express our gratitude to all parties concerned.

REFERENCES

- [1] F. C. Moon, "Superconducting Levitation," Wiley, New York, 1994.
- [2] J. Hull, *Superconductor Science and Technology*, Vol. 13, 2000, p. R1. [doi:10.1088/0953-2048/13/2/201](https://doi.org/10.1088/0953-2048/13/2/201)
- [3] P. T. Putman, Y. X. Zhou, H. Fang, A. Klawitter and K. Salama, *Superconductor Science and Technology*, Vol. 18, 2005, pp. S6-S9. [doi:10.1088/0953-2048/18/2/002](https://doi.org/10.1088/0953-2048/18/2/002)
- [4] S. Y. Wang, J. S. Wang and Z. Y. Ren, *Physica C*, Vol. 386, 2003, pp. 531-535. [doi:10.1016/S0921-4534\(02\)02158-5](https://doi.org/10.1016/S0921-4534(02)02158-5)
- [5] H. H. Wen, X. Y. Zhu, F. Han and G. Mu, *Physical C*, Vol. 470, 2010, pp. s263-s266. [doi:10.1016/j.physc.2010.05.010](https://doi.org/10.1016/j.physc.2010.05.010)
- [6] Z. Deng, J. Wang, J. Zheng, H. Jing, Y. Lu, G. Ma, *et al.*, *Superconductor Science and Technology*, Vol. 21, 2008, Article ID: 115018. [doi:10.1088/0953-2048/21/11/115018](https://doi.org/10.1088/0953-2048/21/11/115018)
- [7] X.-Y. Zhang, J. Zhou and Y.-H. Zhou, *Journal of Applied Physics*, Vol. 107, 2010, Article ID: 036102. [doi:10.1063/1.3291116](https://doi.org/10.1063/1.3291116)
- [8] M. X. Liu and Y. Y. Lu, *Superconductor Science and Technology*, Vol. 24, 2011, pp. 1809-1813. [doi:10.1007/s10948-011-1128-2](https://doi.org/10.1007/s10948-011-1128-2)
- [9] Y. Y. Lu and Y. W. Ge, *Journal of Superconductivity and Novel Magnetism*, Vol. 24, 2011, pp. 1787-1791. [doi:10.1007/s10948-010-1124-y](https://doi.org/10.1007/s10948-010-1124-y)
- [10] Y. Y. Lu and S. J. Zhuang, *Journal of Low Temperature Physics*, Vol. 169, 2012, pp. 111-121. [doi:10.1007/s10909-012-0637-0](https://doi.org/10.1007/s10909-012-0637-0)
- [11] J. S. Wang, S. Y. Wang, Y. W. Zeng, H. Y. Huang and F. Luo, *Physica C*, Vol. 378-381, 2002, pp. 809-814.